

Cite this: *Chem. Commun.*, 2011, **47**, 10100–10102

www.rsc.org/chemcomm

COMMUNICATION

Oriented crystallization of hydroxyapatite by the biomimetic amelogenin nanospheres from self-assemblies of amphiphilic dendrons†

Sheng Yang,^a Hai He,^b Lei Wang,^{*a} Xinru Jia^{*b} and Hailan Feng^{*a}

Received 20th June 2011, Accepted 22nd July 2011

DOI: 10.1039/c1cc13661e

An amphiphilic PAMAM dendron with aspartic acids on the periphery and an aliphatic chain at the focal point was synthesized. The dendrons initially self-assembled to nanospheres in aqueous solution and further translated to linear chains that showed a function similar to amelogenin in the oriented growth of HAP *in vitro*.

As is well known, the mineralized tissues, including cartilage, bone and tooth with special morphologies and excellent biomechanical properties, are developed by the deposition of calcium phosphates on ordered self-assembled proteins.^{1,2} For example, in the oriented growth of enamel crystals, amelogenin, a hydrophobic protein, plays a key role as a highly orchestrated extracellular matrix in the initial step of dental enamel formation (amelogenesis).³ The amelogenin is secreted by ameloblasts and self-organizes into nanospheres that regulate the parallel arrangement of rod-like nano-hydroxyapatite (HAP) crystals. Enamel is the hardest mineralized tissue in vertebrates and cannot regenerate once it is damaged after the elimination of ameloblasts at enamel maturation. Currently, defects in enamel are usually repaired by utilizing many unstructured substitutes like synthetic resins, ceramics and metals which not only do not function as well as the natural one but also have problems integrating with the tissues of the tooth, with ageing, adhesion failure and the materials fracturing. Therefore, the ability to create artificially synthesized materials with enamel-like microstructures for dental therapy is urgently needed.^{4,5}

In order to mimic the biomineralization, many helpful ways, such as peptides,⁶ proteins,⁷ polymer microgels^{8,9} and self-assembling amphiphiles^{10,11} have been developed to ascertain the oriented arrangement of hydroxyapatite crystals in the hard tissues. For example, Stupp and coworkers¹² reported the

self-assembly of peptide amphiphiles into cylindrical micelles that functioned as a template to direct the formation of thin HAP crystals. J. Moradian-Oldak *et al.*⁴ reported the dependence of *c*-axial orientation of hydroxyapatite on the hierarchical self-assembly of birefringent “microribbons” from porcine amelogenins. They suggested that the transition from nanospheres to long chains might be involved in the mechanism of amelogenin as a scaffold in the oriented and elongated growth of apatite crystals.

Inspired by the pioneers' findings, we have been trying to design a PAMAM-based dendritic molecule, with a simple structure and simple synthetic procedures but a facile assembly property, to show novel functions similar to the amelogenins for the oriented and elongated growth of apatite crystals. The obvious advantages are that the dendritic molecules, such as PAMAM dendrimers, closely resemble the topologies and dimensions in the proteins, and the layered structures make them easily modifiable in order to tailor the properties to match various requirements.^{13,14} In addition, our previous studies on the PAMAM dendrons demonstrate their versatile self-assembly behavior with different packing modes caused by changing the focal or periphery groups.^{15,16} Crystallization of HAP in the presence of PAMAM dendrimers has been reported in recent years. For instance, Yang and coworkers^{17,18} reported that the size and shape of HAP nanostructures were effectively influenced by PAMAM with different surface groups, generations and concentrations. Xie *et al.*¹⁹ reported that PAMAM with L-glutamic acid groups on the periphery could affect the crystallization of HAP. However, self-assembly structures from dendritic molecules functioning as amelogenins to direct HAP crystallization are rarely reported.

Herein, we report a novel amphiphilic PAMAM dendritic molecule modified with L-aspartic acids on the periphery and an aliphatic chain at the focal point (Sa-PAMAM-Asp) (Fig. 1). In such a way, we aim to mimic the self-assembly behavior, the function of amelogenins, and the interaction of

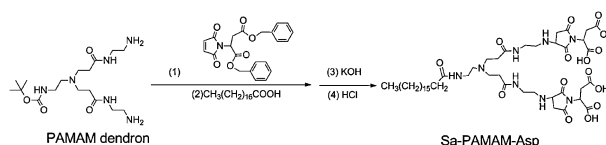


Fig. 1 The modification of PAMAM dendron with aspartic acid and stearic acid.

^a Department of Prosthodontics, Peking University School and Hospital of Stomatology, 22 Zhongguancun Nandajie, Haidian District, Beijing 100081, P. R. China. E-mail: kqfenghl@bjmu.edu.cn; Fax: +86 10 62173402; Tel: +86 10 82195232

^b Beijing National Laboratory for Molecular Sciences, and Key Laboratory of Polymer Chemistry and Physics of the Ministry of Education, College of Chemistry and Molecular Engineering, Peking University, Beijing 100871, P. R. China. E-mail: xrjia@pku.edu.cn; Fax: +86 10 62751708; Tel: +86 10 62752102

† Electronic supplementary information (ESI) available. See DOI: 10.1039/c1cc13661e

aspartic acid residues on the C terminus of amelogenin with apatite *in vitro*.

The PAMAM dendrons ($G = 1$) were synthesized by divergent method and further modified with aspartic acids on the periphery and an aliphatic chain at the focal point (Fig. 1, Sa-PAMAM-Asp). Nuclear magnetic resonance (NMR) technique, electrospray ionization mass spectrometry (ESI-MS) and Fourier transform infrared spectroscopy (FTIR) were used to verify the structure and purity of the obtained compound. The results were in good agreement with the proposed structures and the detailed materials including synthetic procedures and characterization of the amphiphilic dendrons are described in the ESI†

The aggregates of Sa-PAMAM-Asp were prepared by dissolving the sample in dimethyl sulfoxide (DMSO) at room temperature, and then dropping it into aqueous solution at pH 7.4 and 37 °C. The critical aggregation concentration (CAC) of Sa-PAMAM-Asp in aqueous solution was determined by monitoring the change of fluorescence intensity with an increase of the concentration of modified dendrons (Fig. S1 in the ESI†). The CAC value was very low (5.5×10^{-6} M), which coincided with our previous observation for PAMAM dendrimers containing aromatic chromophores on the periphery.¹⁵

The self-assembly of the resulting amphiphilic dendrons in aqueous solution was studied by means of transmission electron microscopy. Fig. 2 shows typical TEM images of the aggregates from Sa-PAMAM-Asp at different concentrations in aqueous solution. Nanospheres of *ca.* 20–50 nm in diameter were initially observed from the samples with concentrations around the CAC, such as 6.0×10^{-6} M (Fig. 2a). However, the nanospheres were not thermodynamically stable. After the sample was kept in aqueous solution at 37 °C for 2 days, short linear chains of *ca.* 20–30 nm in width and 100–200 nm in length were clearly observed, indicating a process of fusion of the nanospheres, resulting in a stable state (Fig. 2b). In addition, linear chains of 30–50 nm in diameter and 20–500 nm in length could also be generated with the increase of concentration (*e.g.* up to 1.6×10^{-4} M). In this case, nanospheres could not be observed from the freshly prepared samples (Fig. S2 in the ESI†). In order to facilitate the linear fabrication of the dendrons, 0.1 M $\text{Ca}(\text{NO}_3)_2$ was added as an additive into the system for the reason that it was an effective way to alter the morphology of supramolecular assemblies by changing the microenvironment as reported in the literature.^{20,21} The longer linear chains (300 nm–1.5 μm in length)

resulted from the fusion of nanospheres (40 nm in diameter, inset of Fig. 2c) could also be obtained in the presence of 0.1 M $\text{Ca}(\text{NO}_3)_2$ and 1.6×10^{-4} M Sa-PAMAM-Asp (Fig. 2c). Such self-assembly behavior is similar to our previous study on the PAMAM dendrons focally modified with aromatic chromophores.¹⁶ The driving forces in the assemblies include H-bonding of amides in the branches, carboxyl groups on the periphery, and hydrophobic interactions of the aliphatic chain at the focal point. Structurally, flexible hydrophilic dendritic branches and the carboxyl groups are located in the outer layer of the aggregates, leading to nanospheres that are very adhesive. They are readily attached by H-bonding interaction and the entanglement of the branches, which leads to the formation of linear chains by the fusion of several individuals. The entanglement of branches, the H-bonding of carboxyl groups and amide groups in the branches would strengthen the contact of the assemblies, leading to fusion of nanospheres to form linear chains (Fig. S3†).

The resulting assemblies resemble amelogenin in morphology and structural residues of aspartic acid, which may create an ideal environment for the oriented growth of apatite crystals *in vitro*. Encouraged by this, we then used the assemblies of Sa-PAMAM-Asp in aqueous solution for the mineralization of HAP (for detailed procedures see ESI†) at pH = 7.4 and 37 °C. It was found that the HAP crystals displayed quite a different morphology as compared to the plate-like crystals (100–600 nm in length and 50–100 nm in wide) developed in the absence of the aggregates (Fig. S4 in the ESI†). As showed in Fig. 3a, bundles of oriented crystals of 10–50 nm in width and 110–700 nm in length were observed in the TEM images. Remarkably, the crystals arrayed approximately along the linear chains and each bundle contained several parallel filaments of 3–4 nm in width and 100–500 nm in length (Fig. 3b and Fig. S7 in the ESI†). Such structures are consistent with reported parallel filaments obtained by adding the recombination amelogenin into calcifying solution.^{3,22,23}

The calcium-phosphorus molar ratio (Ca/P) of the resulting crystals was analyzed by energy dispersion from an X-ray detector (EDX). By careful observation, we found that a metastable amorphous calcium phosphate (ACP) with a Ca/P molar ratio of *ca.* 1.5 took shape rapidly in the initial stage (in 7 days, inset of Fig. 3a), and it transformed to the stable apatite crystals in 14 days with a Ca/P molar ratio of *ca.* 1.67 (inset of Fig. 3d). Fig. 3c and f show the electron diffraction patterns of regions in images (a) and (b) respectively, and the typical reflections of HAP are marked with (002), (211) and (210). The electron diffraction patterns indicated the parallel alignment of oriented and elongated apatite crystals, similar to the enamel rods.²⁴ As shown in Fig. 3e, the spacing of crystal lattice along the long axis is 0.346 nm (selected region from Fig. 3d, marked with red frame) which corresponded to the (002) face of HAP crystals as reported in the literature.²³ To develop a better understanding of the crystals, XRD measurement was used to further verify its structure. A peak appeared at $2\theta = 25.9^\circ$ which was the characteristic (002) diffraction of HAP (Fig. S9a in the ESI†). This peak was enhanced as compared with that of the crystals formed without assemblies (Fig. S9b in the ESI†), suggesting that the apatite developed preferentially along the *c*-axis to some extent.

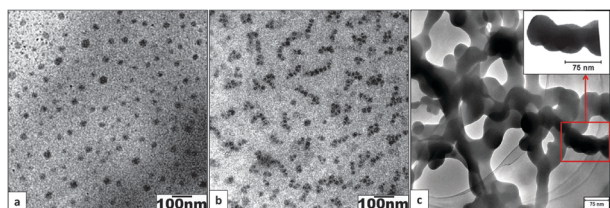


Fig. 2 TEM images of the aggregates of Sa-PAMAM-Asp: (a) the nanospheres at a concentration of 6.0×10^{-6} M; (b) the short chains of fusing nanospheres as time goes on (2 days); (c) the linear chains of the amphiphilic dendrons at a concentration of 1.6×10^{-4} M in the presence of 0.1 M $\text{Ca}(\text{NO}_3)_2$.

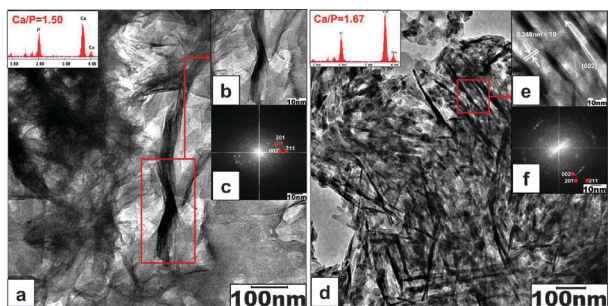


Fig. 3 The high-resolution TEM images of (a) the oriented growth of HAP crystals in the presence of linear chains from Sa-PAMAM-Asp (7 days). (b) TEM image of a mineralized bundle of filaments assembled parallel to their *c*-axis (selected from image (a), marked with red frame); (c) electron diffraction pattern of a region taken from image (a), typical reflections of HAP are marked; (d) HAP crystals in the presence of linear chains from Sa-PAMAM-Asp (14 days). (e) The spacing of the crystal lattice along the long axis (selected from image (d), marked with red frame). Long white arrow indicates the long axis direction of the microstructures. (f) Electron diffraction pattern of a region taken from image (d), typical reflections of HAP are marked.

In the experiments, we found that ions of Ca^{+2} were initially deposited on the linear chains (Fig. S5 in the ESI†) by chelating with carboxyl groups on the assemblies, then grew along the long axis and finally generated the ordered crystals. This reflects that the assemblies selectively adsorb to the *a/b* crystallographic planes, functioning similarly to amelogenins during the enamel mineralization.^{25,26} We therefore speculated that the oriented crystallization of HAP in our study originated from the linear chains of the hierarchical assembly of the nanospheres in which the alkyl tails packed in the center through hydrophobic interaction, while the carboxyl groups of Asp arranged at the outer edge of the assemblies. As proposed in the literature,⁴ the fabrication of “tubular sheaths” is crucial in the development of the ordered array of inorganic crystals in a prism, and the collinear arrays of amelogenin nanospheres initiated the early stage of mineral deposition.³ Moreover, it is a common sense that the ordered arrangement of acidic functional groups fulfils the key structural role in the biomineralization world, such as the regular hydrophobic/hydrophilic domains of amelogenin afford an oriented alignment of acidic peptides on a hydrophobic substrate. From these points of view, the linear assemblies match the essentials of biomineralization so as to resemble the function of amelogenin.

In conclusion, the self-assembly behavior of a novel amphiphilic dendron Sa-PAMAM-Asp in aqueous solution was investigated. Sa-PAMAM-Asp self-assembled into nanospheres initially and further translated into linear chains either by increasing the concentration or by adding an additive. The linear assemblies showed a function similar to amelogenin in the oriented growth of HAP. It was found that the apatite developed in the presence of the linear assemblies resembled some of the features of the lowest level of the hierarchical structure of enamel, such as the preferential orientation of the *c*-axis of the HAP crystals along the amelogenin aggregates. To the best of our knowledge, this is a rare example of

fabricating the oriented HAP with synthetic dendritic molecules. The present work provides direct experimental evidence for the protein-mediated HAP nucleation and growth and it may also reveal the mechanism involved in enamel biomineralization.

The authors thank Jing Chen, Mingjun Teng for TEM and EDS characterization, Fuhui Liao for XRD analysis, and Ming Gao for CAC tests. The authors are most grateful to all reviewers of this article for their comments and suggestions. The work is supported by the National Natural Science Foundation of China (NSFC Grant 30572063 and 30600717) and the Doctoral Fund of Ministry of Education of China (20070001726).

Notes and references

- 1 L. B. Gower, *Chem. Rev.*, 2008, **108**, 4551–4627.
- 2 A. George and S. Ravindran, *Nano Today*, 2010, **5**, 254–266.
- 3 X. Yang, L. Wang, Y. Qin, Z. Sun, Z. J. Henneman, J. Moradian-Oldak and G. H. Nancollas, *J. Phys. Chem. B*, 2010, **114**, 2293–2300.
- 4 C. Du, G. Falini, S. Fermani, C. Abbott and J. Moradian-Oldak, *Science*, 2005, **307**, 1450–1454.
- 5 M. Hannig and C. Hannig, *Nat. Nanotechnol.*, 2010, **5**, 565–569.
- 6 K. Ohkawa, S. Hayashi, N. Kameyama, H. Yamamoto, M. Yamaguchi, S. Kimoto, S. Kurata and H. Shinji, *Macromol. Biosci.*, 2009, **9**, 79–92.
- 7 W. Zhang, S. S. Liao and F. Z. Cui, *Chem. Mater.*, 2003, **15**, 3221–3226.
- 8 S. Schachschal, A. Pich and H. J. Adler, *Langmuir*, 2008, **24**, 5129–5134.
- 9 S. Schweizer and A. Taubert, *Macromol. Biosci.*, 2007, **7**, 1085–1099.
- 10 H. Chen, B. H. Clarkson, K. Sun and J. F. Mansfield, *J. Colloid Interface Sci.*, 2005, **288**, 97–103.
- 11 C. E. Fowler, M. Li, S. Mann and H. C. Margolis, *J. Mater. Chem.*, 2005, **15**, 3317–3325.
- 12 J. D. Hartgerink, E. Beniash and S. I. Stupp, *Science*, 2001, **294**, 1684–1688.
- 13 D. A. Tomalia, *Prog. Polym. Sci.*, 2005, **30**, 294–324.
- 14 R. Esfand and D. A. Tomalia, *Drug Discovery Today*, 2001, **6**, 427–436.
- 15 B. B. Wang, X. Zhang, X. R. Jia, Z. C. Li, Y. Ji, L. Yang and Y. Wei, *J. Am. Chem. Soc.*, 2004, **126**, 15180–15194.
- 16 B. B. Wang, W. S. Li, X. R. Jia, M. Gao, Y. Ji, X. Zhang, Z. C. Li, L. Jiang and Y. Wei, *J. Colloid Interface Sci.*, 2007, **314**, 289–296.
- 17 F. Zhang, Z. H. Zhou, S. P. Yang, L. H. Mao, H. M. Chen and X. B. Yu, *Mater. Lett.*, 2005, **59**, 1422–1425.
- 18 Z. H. Zhou, P. L. Zhou, S. P. Yang, X. B. Yu and L. Z. Yang, *Mater. Res. Bull.*, 2007, **42**, 1611–1618.
- 19 L. B. Xie, L. Wang, X. R. Jia, G. C. Kuang, S. Yang and H. L. Feng, *Polym. Bull.*, 2011, **66**, 119–132.
- 20 T. Lu, F. Han, Z. C. Li, J. B. Huang and H. L. Fu, *Langmuir*, 2006, **22**, 2045–2049.
- 21 T. Shimizu, M. Masuda and H. Minamikawa, *Chem. Rev.*, 2005, **105**, 1401–1443.
- 22 E. Beniash, J. P. Simmer and H. C. Margolis, *J. Struct. Biol.*, 2005, **149**, 182–190.
- 23 L. Wang, X. Guan, C. Du, J. Moradian-Oldak and G. H. Nancollas, *J. Phys. Chem. C Nanomater. Interf.*, 2007, **111**, 6398–6404.
- 24 M. J. Glimcher, E. J. Daniel, D. F. Travis and S. Kamhi, *J. Ultrastruct. Res.*, 1965, **S**, 14.
- 25 A. G. Fincham, J. Moradian-Oldak and J. P. Simmer, *J. Struct. Biol.*, 1999, **126**, 270–299.
- 26 H. C. Margolis, E. Beniash and C. E. Fowler, *J. Dent. Res.*, 2006, **85**, 775–793.